

**One-dimensional conduction through supporting electrolytes:  
Two-scale cathodic Debye-layer**

Yaniv Almog

*Department of Mathematics*

*Louisiana State University*

Ehud Yariv

*Department of Mathematics*

*Technion — Israel Institute of Technology*

## Abstract

Supporting-electrolyte solutions comprise of chemically inert cations and anions, produced by salt dissolution, together with a reactive ionic species which may be consumed and generated on bounding ion-selective surfaces (e.g. electrodes or membranes). Upon application of external voltage, a Faraday current is thereby established. It is natural to analyze this ternary-system process through a one-dimensional transport problem, employing the thin Debye-layer limit. Using a simple model of ideal ion-selective membranes, we have recently addressed this problem for moderate voltages (*Phys. Rev. Lett.*, vol. 105, 2010, 176101), predicting currents that scale as a fractional power of Debye thickness. We here address the complementary problem of moderate currents.

We employ matched asymptotic expansions, separately analyzing the two “inner” thin Debye layers adjacent to the ion-selective surfaces and the “outer” electro-neutral region outside them. A straightforward calculation following comparable singular-perturbations analyses of binary systems is frustrated by the prediction of negative ionic concentrations near the cathode. Accompanying numerical simulations, performed for small values of Debye thickness, indicate a number unconventional features occurring at that region, such as inert-cation concentration amplification and electric-field intensification. The current–voltage correlation data of the electro-chemical cell, obtained from compilation of these simulations, does not approach a limit as the Debye thickness vanishes.

Resolution of these puzzles reveals a transformation of the asymptotic structure of the cathodic Debye layer. This reflects the emergence of an internal boundary layer, adjacent to the cathode, wherein field and concentration scaling differs than that of the Gouy–Chapman theory. The two-scale feature of the cathodic Debye layer is manifested through a logarithmic voltage scaling with Debye thickness. Accounting for this scaling, the compiled current–voltage data collapses upon a single curve. This curve practically coincides with an asymptotically calculated universal current–voltage relation.

## I. INTRODUCTION

### A. Background

The analysis of ionic conduction in electrolyte solutions is a classical problem in electrochemistry [1] which now receives renewed interest in such areas as thin-film batteries [2], biological membranes [3], desalination systems [4], and microfluidic devices [5], where appropriate components (electrodes, ionic channels, perm-selective membranes and nanochannel arrays) function as ion-selective surfaces. For practical purposes, it is desired to derive a lumped representation of the conduction process via approximate current–voltage relations [6], preferably in a universal form independent of the Debye length [7, 8].

Typically, this process is modeled using a one-dimensional transport problem comprising an electrolyte solution bounded by two ion-selective surfaces (e.g. membranes or electrodes). For simplicity, it has been customary to analyze binary solutions, typically with “inert” anions and “reactive” cations. On a continuum level the bounding surfaces are represented by an impermeability condition for the anionic species together with an appropriate model of the ion-selective surface. The simplest model is that of ideal membrane, where the reactive species concentration is simply specified [4, 7, 9, 10].

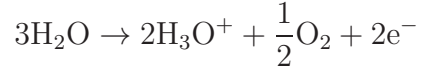
When a voltage is applied across the two surfaces, Faraday current is generated. In analyzing this problem in the Poisson–Nernst–Planck framework, the smallness of Debye thickness as compared with device size naturally leads to a boundary-layer description, with the electrolyte solution being approximately electro-neutral outside two narrow boundary (“Debye”) layers adjacent to the bounding ion-exchange surfaces [9, 11].

The passage of current results in an inherent asymmetry. Thus, The absence of anionic flux necessitates concentration polarization at the electro-neutral region [12], wherein both cationic and anionic concentration vary linearly along the cell, with concentration enrichment near the anode and depletion near the cathode [9, 11].

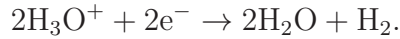
### B. Supporting electrolytes

Many real systems comprise more than two ionic species. Typically, the salt molecules in the solution dissolve into cations and anions that cannot discharge on the bounding surfaces. These two inert species constitute a “supporting-electrolyte”; their total amount is fixed.

The surfaces can nevertheless interact with a third type of ions, whose total number is non-restricted. An example of such a reactive ion is hydronium, which is generated at the anode via water dissociation



and consumed at the cathode via the recombination



The reactions take place in the presence of an indifferent electrolyte, say KCl (see [13]), which serves as the supporting electrolyte. Other examples of supporting-electrolyte systems include (i) water electrolysis using a sodium sulfate solution; and (ii) two Ag/AgCl electrodes immersed in an electrolyte solution of water and Ammonium Nitrate. In the latter case the chemical reaction entails Chloride-anion liberation at the cathode, and its absorption at the anode (a small amount of some chloride salt has to be added to the solution to initiate the process).

As in the existing literature of binary systems, ternary systems have been analyzed within the Nernst–Planck–Poisson framework [14]. In the thin double-layer limit, asymptotic investigations have relied upon the assumption of *different* amounts of inert cations and ions [15]. This results in mathematical structure which closely resembles that in comparable binary systems [11]. It is however experimentally known [16] that ternary systems exhibit a qualitatively different behavior from their binary counterparts. Specifically, the presence of supporting electrolyte leads to low concentration of reactive ions and a concomitant current mitigation. Moreover, while the assumption of different amounts of inert ions may be appropriate to various situations, it appears natural to consider the case of *identical* amounts, corresponding to the above examples of supporting electrolytes.

It turns out that the latter case lead to a rather unconventional asymptotic structure. Thus, while in binary systems  $O(1)$  voltages lead to  $O(1)$  currents [11], the behavior of supporting-electrolyte systems turn out more complicated. In a recent analysis [17] we have demonstrated that moderate  $O(1)$  voltages result in an asymptotically small current that scales as the 2/3-power of the Debye width. This current abatement is consistent with reported experimental observations [16].

It is natural then to consider the complementary problem of moderate *currents* in ternary solutions. Given the nature of the above-mentioned small-current problem, it is anticipated

that the required voltage would be large, in some asymptotic sense. It is however *a priori* unclear how it would scale. Answering this question, and understanding the physical mechanism underlying the transport process, together constitute the goal of the present paper.

The paper is arranged as follows. In the next section we formulate the governing equation. The thin Debye-layer limit is addressed in Sec. III, where we demonstrate how the use of singular perturbations leads to the paradoxical prediction of negative ionic concentrations. The paradox is resolved in Sec. IV, where we identify the need for a delicate analysis near the cathode. The resulting current–voltage relation is derived in Sec. V; in that section we also illustrate the emergence of an internal boundary layer. We conclude in Sec. VI.

## II. PROBLEM FORMULATION

A conceptual electrochemical cell comprises an electrolyte solution (permittivity  $\epsilon_*$ ) bounded by two ion-selective membranes spaced a distance  $L_*$  apart (variables decorated with an asterisk subscript denote hereafter dimensional quantities). The solution consists of two “inert” ionic species (initially formed by salt dissociation) which do not discharge on the membranes, and a third (say positive) “reactive” species, which can discharge there. For simplicity, all ionic species are presumed univalent.

At time zero, a constant voltage is applied to the bounding surfaces. Following a short transient period, a steady-state one-dimensional charge transport is established. Our interest lies in the current–voltage relation characterizing this state. We employ a dimensionless notation where length variables are normalized by  $L_*$ , ionic concentrations by a reference concentration  $c_*$  (to be specified later on), and electric potentials and fields by the respective thermal scales  $\varphi_* = R_*T_*/F_*$  ( $R_*$  being the gas constant,  $T_*$  the absolute temperature, and  $F_*$  Faraday constant) and  $\varphi_*/L_*$ . In that notation, the inert concentrations are denoted by  $c_{\pm}$ , the reactive-species concentration by  $r$ , and the electric field by  $e$ . The cathode at  $x = 0$  is maintained at a negative electric potential  $-V$  relative to the anode at  $x = 1$ .

At steady-state one-dimensional transport, ionic conservation implies spatially uniform fluxes for all ionic species. Due to ionic impermeability at the ion-selective surfaces, the flux of the two inert species must vanish identically. This is expressed by the following integrals

of the Nernst–Planck equations:

$$-\frac{dc_+}{dx} + c_+e = 0, \quad -\frac{dc_-}{dx} - c_-e = 0. \quad (1)$$

The reactive species, on the other hand, experiences in general a non-zero flux (normalized by  $D_*c_*/L_*$ ,  $D_*$  being its diffusivity), say  $4j$  [18], directed towards the cathode (in the negative- $x$  direction)

$$-\frac{dr}{dx} + re = -4j. \quad (2)$$

The electric field, in turn, is governed by Poisson’s equation

$$c_+ - c_- + r = 2\delta^2 \frac{de}{dx}. \quad (3)$$

Here

$$\delta = \lambda_*/L_* \quad (4)$$

is the dimensionless Debye width, with  $\lambda_* = (\epsilon_*\varphi_*/2F_*c_*)^{1/2}$ .

The preceding differential equations are supplemented by appropriate boundary conditions. The no-flux condition governing the inert species is already implicit in (1). Following [4, 7, 9, 10], we employ the ideal-membrane model, prescribing a fixed concentration of the reactive species,

$$r = p \quad \text{at} \quad x = 0, 1. \quad (5)$$

In addition to these conditions, several integral conditions must be imposed. Thus, the external voltage application appears as

$$\int_0^1 e \, dx = -V, \quad (6)$$

while the initial condition of the system is manifested via the following “memory constraints” [11, 14, 15], specifying the total amount of inert ions:

$$\int_0^1 c_+ \, dx = 1, \quad \int_0^1 c_- \, dx = 1. \quad (7)$$

These constraints represent the invariance of that amount during the unsteady transient phase which follows voltage activation. As such, they effectively define  $c_*$  as the average (dimensional) concentration of either inert species at time zero.

In principle, the preceding potentiostatic problem determines  $j$  and the four fields [ $c_{\pm}(x)$ ,  $r(x)$ , and  $e(x)$ ] as functions of  $V$ ,  $\delta$ , and  $p$ . Following the standard practice [11], we address

the equivalent galvanostatic problem, seeking to obtain  $V$  for a prescribed value of  $j$ . Note that  $4j$  constitutes here the electric current towards the cathode, normalized by  $F_*D_*c_*/L_*$ .

While no analytic closed-form solution for the above problem are available, it is noteworthy that equations (1) imply Boltzmann distributions for  $c_{\pm}$ :

$$c_{\pm} \propto e^{\mp\varphi}, \quad (8)$$

whereby

$$c_+c_- = \text{const.} \quad (9)$$

### A. Alternative formulation

It is sometimes convenient to employ the alternative variables [cf. [11]]

$$c = c_+ + c_- + r, \quad q = c_+ - c_- + r, \quad (10)$$

respectively corresponding to the mean (“salt”) ionic concentration and volumetric charge density. Addition and subtraction of (1)–(2) respectively yield the salt

$$\frac{dc}{dx} - qe = 4j \quad (11)$$

and charge

$$\frac{dq}{dx} - ce = 4j. \quad (12)$$

balances. In terms of  $c$  and  $q$ , Poisson’s equation (3) appears as

$$q = 2\delta^2 \frac{de}{dx} \quad (13)$$

while the memory conditions (7) yields

$$\int_0^1 (c - q) dx = 2. \quad (14)$$

Following binary-system analyses [19, 20] the preceding equations can be captured by a single master equation (see [17]): substitution of (13) into (11) followed by integration yields the salt concentration

$$c = 4jx + \delta^2 e^2 + G. \quad (15)$$

Here,  $G$  is a positive integration constant; it is found by substituting into the normalization condition (14) in conjunction with (13):

$$G = 2 - 2j + \delta^2 \left[ 2e(x=1) - 2e(x=0) - \int_0^1 e^2 dx \right]. \quad (16)$$

Then, substitution of (13) and (15) into (12) provides an independent differential equation governing the electric field

$$2\delta^2 \frac{d^2 e}{dx^2} - e(4jx + \delta^2 e^2 + G) = 4j. \quad (17)$$

### III. THIN DEBYE-LAYER LIMIT

Since all practical systems are characterized by thin double layers, we hereafter focus upon the asymptotic limit

$$\delta \ll 1. \quad (18)$$

Our goal is the analysis of the transport problem in that limit. Specifically, we are interested in obtaining a useful approximation for the  $j$ - $V$  relation characterizing that problem.

#### A. Numerical solution

Equations (1)–(7) are easily recast as a boundary-value problem that is solved using standard shooting methods. In solving the equivalent galvanostatic problem, we integrate the differential equations to obtain the pertinent fields for a given  $j$ , and then calculate  $V$  using (6).

Using that approach, we have numerically calculated the functional relation between  $j$  and  $V$  for several  $\delta$  values, using  $p = 2$ . The results are shown in Fig. 1. Despite the small  $\delta$  values, the respective sets of data points do not seem to approach a limiting curve. This feature is unfamiliar in corresponding studies of binary electrolytes, see for example fig. 2 of Ref. [11].

#### B. Inner-outer expansions

In what follows we attempt to obtain analytic approximations for the transport processes in the cell which would, *inter alia*, explain the scatter appearing in Fig. 1. To this end,

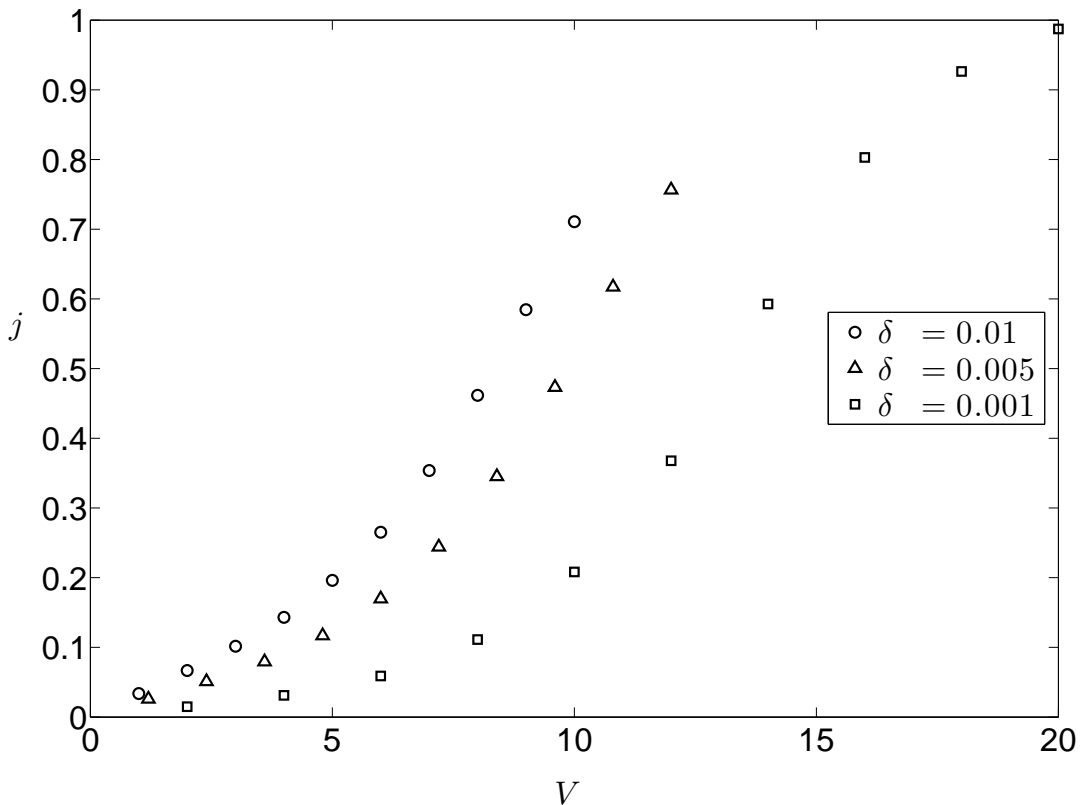


FIG. 1. Numerical current–voltage correlations for the indicated  $\delta$  values (with  $p = 2$ ).

we employ perturbation methods. It is well known [4, 11] that the limit (18) is singular, leading to an asymptotic decomposition of the electrolyte domain into three asymptotic regions: two  $O(\delta)$ -thick boundary (“Debye”) layers adjacent to the ion-selective surfaces, where  $e \sim O(\delta^{-1})$ , as well as an approximately electro-neutral “outer” region, where all fields are  $O(1)$ . Different scalings and approximations are used in each region, with appropriate matching conditions connecting them.

### 1. Outer region

The outer-region variables are decorated by a bar accent. The outer coordinate  $\bar{x}$  cannot delineate the behavior within the narrow Debye layers, and hence the outer solution at  $\bar{x} = 0, 1$  does not satisfy the boundary conditions on the literal ion-selective surfaces  $x = 0, 1$ . Instead, we match it with the outer edges of the Debye-layer solution as  $\bar{x} \rightarrow 0, 1$ .

To leading-order, the outer solution is obtained by neglecting  $o(1)$  terms in the governing equations. Poisson's equation (3) then yields the familiar electro-neutrality

$$q = 0 \tag{19}$$

while from Eq. (17) we obtain the electric field

$$\bar{e} = -\frac{4j}{G + 4j\bar{x}}. \tag{20}$$

Substitution into the Nernst–Planck equations (1) yields the concentrations

$$\bar{c}_+ = \frac{H_+}{G + 4j\bar{x}}, \quad \bar{c}_- = H_-(G + 4j\bar{x}), \tag{21}$$

in which  $H_{\pm}$  are integration constants. Use of (2), (15) and (20) reveals that  $H_- = 1/2$  and

$$\bar{r} = \frac{G + 4j\bar{x}}{2} - \frac{H_+}{G + 4j\bar{x}}, \tag{22}$$

The integration constants  $G$  and  $H_+$  are to be found by matching with the boundary layer fields.

## 2. Cathodic Debye layer

Consider next the cathodic boundary layer about  $x = 0$ , described by the stretched coordinate

$$X = x/\delta. \tag{23}$$

As is frequently assumed when studying similar problems [4] we postulate  $O(1)$  concentrations,

$$c_{\pm}(x; \delta) \approx C_{\pm}(X) + \dots, \quad r(x; \delta) \approx R(X) + \dots, \tag{24}$$

and an  $O(\delta^{-1})$  electric field,

$$e(x; \delta) \approx \delta^{-1}E(X) + \dots. \tag{25}$$

Using (17), the leading-order electric field satisfies the differential equation,

$$2\frac{d^2E}{dX^2} - E^3 - GE = 0. \tag{26}$$

Since the outer field (20) is regular as  $x \rightarrow 0$ , the scaling (25) implies that  $E$  must vanish at large  $X$ . Integration of (26) in conjunction with that condition readily yields

$$E = -\frac{2^{1/2}G^{1/2}}{\sinh\{2^{-1/2}G^{1/2}(X + X_0)\}}, \tag{27}$$

where  $X_0$  is an integration constant. Use of the Nernst–Planck equations (1) and the required matching with (21) readily provides the ionic concentration:

$$C_+ = \frac{H_+}{G} \coth^2 \{8^{-1/2} G^{1/2} (X + X_0)\}, \quad (28)$$

$$C_- = \frac{G}{2} \tanh^2 \{8^{-1/2} G^{1/2} (X + X_0)\}. \quad (29)$$

Within the narrow Debye layer the reactive species satisfy the same leading-order equation as that governing the positive inert species [cf. (1)–(2)]. Matching with (22) therefore yields

$$R = \left( \frac{G}{2} - \frac{H_+}{G} \right) \coth^2 \{8^{-1/2} G^{1/2} (X + X_0)\}. \quad (30)$$

Application of boundary condition (5),  $R(0) = p$ , then furnishes the relation

$$\coth^2 \{8^{-1/2} G^{1/2} X_0\} = \frac{2pG}{G^2 - 2H_+}. \quad (31)$$

### 3. Anodic Debye layer

The structure of the anodic boundary layer about  $x = 1$  is obtained in a similar manner, now with

$$X = \frac{1 - x}{\delta}. \quad (32)$$

The comparable fields, denoted  $\tilde{E}$ ,  $\tilde{C}_\pm$  and  $\tilde{R}$ , are respectively provided by the functions  $-E$ ,  $C_\pm$ , and  $R$ , with  $G$  replaced by  $G + 4j$  [see (21)] and  $X_0$  by a new integration constant  $\tilde{X}_0$ :

$$\tilde{E} = \frac{2^{1/2}(G + 4j)^{1/2}}{\sinh \left\{ 2^{-1/2}(G + 4j)^{1/2}(X + \tilde{X}_0) \right\}}, \quad (33)$$

$$\tilde{C}_+ = \frac{H_+}{G + 4j} \coth^2 \left\{ 8^{-1/2}(G + 4j)^{1/2}(X + \tilde{X}_0) \right\}, \quad (34)$$

$$\tilde{C}_- = \frac{G + 4j}{2} \tanh^2 \left\{ 8^{-1/2}(G + 4j)^{1/2}(X + \tilde{X}_0) \right\}, \quad (35)$$

$$\tilde{R} = \left( \frac{G + 4j}{2} - \frac{H_+}{G + 4j} \right) \coth^2 \left\{ 8^{-1/2}(G + 4j)^{1/2}(X + \tilde{X}_0) \right\}. \quad (36)$$

Kinetic condition (5) now yields

$$\coth^2 \left\{ 8^{-1/2}(G + 4j)^{1/2} \tilde{X}_0 \right\} = \frac{2p(G + 4j)}{(G + 4j)^2 - 2H_+}. \quad (37)$$

### C. Paradox

Following the standard practice in similar binary systems [11], the integration constants are obtained from the memory conditions (7). Since the Debye-layer concentrations are presumably  $O(1)$ , the leading-order contribution to conditions (7) is expected to be determined exclusively by the outer region. At leading order, conservation (7) of inert anions then reads:

$$\int_0^1 \bar{c}_- d\bar{x} = 1. \quad (38)$$

Substitution of (21) therefore yields [cf. (16)]

$$G = 2 - 2j. \quad (39)$$

Note that (15) and (39) imply  $j < 1$ , with the saturation value  $j = 1$  corresponding to zero concentration at the cathode. This mechanism of diffusion-limited current is familiar from the analysis of binary systems [4, 7, 11].

We now repeat the above procedure for the inert-cation species, with

$$\int_0^1 \bar{c}_+ d\bar{x} = 1. \quad (40)$$

Here, substitution of (21) in conjunction with (39) yields

$$\int_0^1 \bar{c}_+ d\bar{x} = \frac{H_+}{4j} \ln \frac{1+j}{1-j}, \quad (41)$$

whereby (40) provides the value

$$H_+ = \frac{4j}{\ln(1+j) - \ln(1-j)}. \quad (42)$$

With that value, however, the reactive concentration (22) becomes, using (39),

$$\bar{r} = 1 - j + 2j\bar{x} - \frac{2j}{(1-j + 2j\bar{x}) \ln \frac{1+j}{1-j}}. \quad (43)$$

This expression is *negative* at the neighborhood of  $\bar{x} = 0$  for all  $0 < j < 1$ . We have clearly encountered a paradox.

### IV. RESOLUTION

To understand where the above procedure fails, it is expedient to inspect the numerical solution in more detail. For small values of  $\delta$  the numerical solution indeed exhibits two

$O(\delta)$ -thick boundary layers near  $x = 0, 1$ . In contrast to the Debye scaling (24), however,  $c_+$  behaves differently at each layer, displaying a pronounced orders-of-magnitude asymmetry. Thus, the cathodic region is characterized by large concentration of inert cations, as opposed to the anodic region, where that concentration is moderate. That asymmetry is illustrated in Fig. 2 for  $\delta = 0.01$  (note the logarithmic scale).

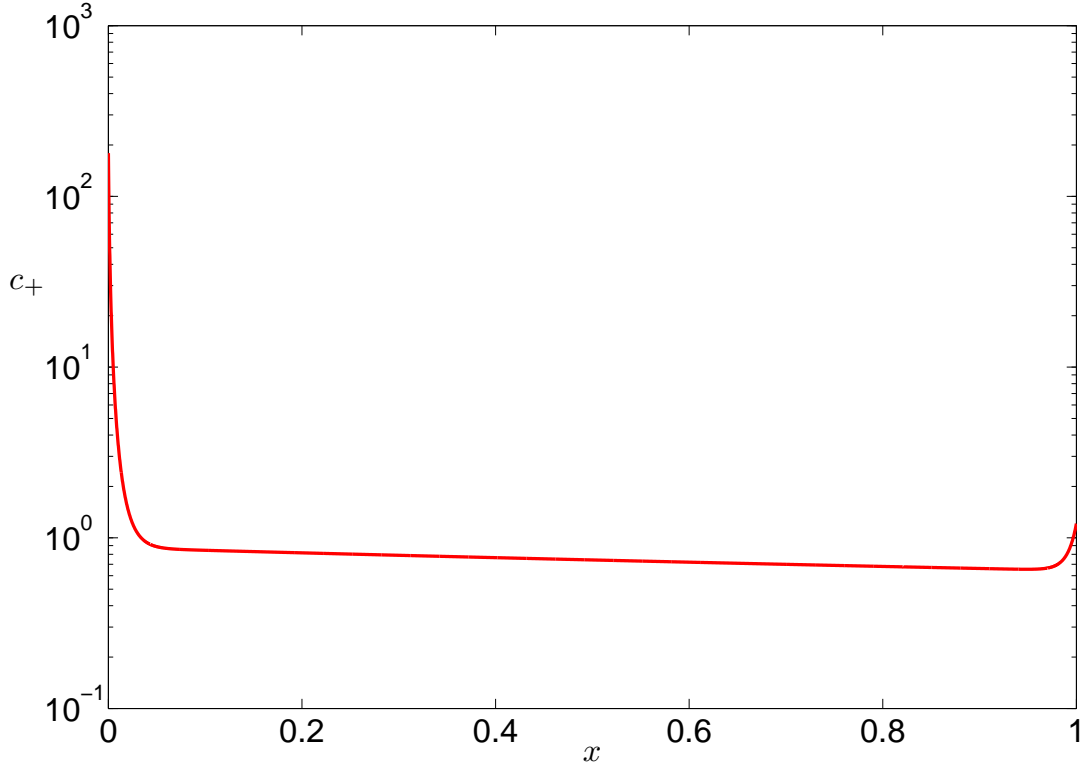


FIG. 2. Cathodic-Debye-layer amplification, demonstrated by the distribution of the numerically calculated inert cationic concentration ( $\delta = 0.01$ ,  $p = 1$ ,  $V = 5$ ).

The numerical results behoove us to carefully scrutinize the Debye-layer analysis. In view of (29),  $c_-$  is bounded as  $\delta \rightarrow 0$  within the boundary layers. Thus, (38) is valid, as is then (39). In contrast, (28) allows for diverging values of  $c_+$  as  $X_0 \rightarrow 0$  or  $\tilde{X}_0 \rightarrow 0$ . Specifically, the presumed  $O(\delta)$  Debye-layer contribution to the cationic memory condition may become  $O(1)$  if either  $X_0$  or  $\tilde{X}_0$  is  $O(\delta)$ . This singular dependence upon  $\delta$  cannot be captured by

the naive expansions (24)–(25), which must be replaced by the *generalized* expansions

$$c_{\pm}(x; \delta) \approx C_{\pm}(X; \delta) + \dots, \quad r(x; \delta) \approx R(X; \delta) + \dots, \quad (44)$$

$$e(x; \delta) \approx \delta^{-1}E(X; \delta) + \dots, \quad (45)$$

where the (possibly singular) dependence upon  $\delta$  of the leading-order fields is introduced through integration constants.

The flaw in the present analysis is therefore pinned at (40): the cationic memory integral is dominated by *both* the outer contribution (41) as well as a cathodic Debye-layer contribution. The calculation of the latter must be done with care, since the integral of  $C_+(X)$  diverges on the interval  $(0, \infty)$ . We therefore rewrite the cationic memory condition in the form [cf. (21) and (41)]

$$\int_0^1 \left\{ c_+(x) - \frac{H_+}{G + 4jx} \right\} dx = 1 - \frac{H_+}{4j} \ln \frac{G + 4j}{G}. \quad (46)$$

Clearly, the outer contribution to the left-hand-side integral is  $o(1)$ . The leading-order contributions from the cathodic and anodic Debye layers appear now as convergent integrals which respectively yield, upon using (39),

$$\int_0^{\infty} \left\{ C_+(X) - \frac{H_+}{G} \right\} dX = \frac{2\delta(1-j)^{-3/2}H_+}{e^{X_0\sqrt{1-j}} - 1}, \quad (47)$$

$$\int_0^{\infty} \left\{ \tilde{C}_+(X) - \frac{H_+}{G + 4j} \right\} dX = \frac{2\delta(1+j)^{-3/2}H_+}{e^{\tilde{X}_0\sqrt{1+j}} - 1}. \quad (48)$$

It is readily seen from (31), (37) and (39) that the only possible solution is with  $X_0 = O(\delta)$  while  $\tilde{X}_0 = O(1)$ . We accordingly define

$$X_0 = \delta\xi_0 \quad (49)$$

with  $\xi_0 = O(1)$ . It then follows from (31) that to leading order

$$H_+ = \frac{G^2}{2}, \quad (50)$$

replacing the wrong result (42). The cathodic-layer contribution (47) then becomes  $4/\xi_0$  [while the anodic-layer contribution (48) is  $O(\delta)$ ]. Replacing the left-hand-side of (46) with that expression yields at leading order

$$\xi_0 = \frac{4}{g(j)} \quad (51)$$

where

$$g(j) = 1 - \frac{(1-j)^2}{2j} \ln \frac{1+j}{1-j} \quad (52)$$

is a function of  $j$  alone, positive for  $0 < j < 1$ .

In view of (39) and (50), multiplication of (21) yields at leading order  $\bar{c}_+ \bar{c}_- = (1-j)^2$ . In view of (9), this relation holds in the entire domain [cf. (28)–(29)]:

$$c_+ c_- = (1-j)^2. \quad (53)$$

## V. CURRENT–VOLTAGE RELATION AND INTERNAL BOUNDARY LAYER

### A. Current–voltage relation

We can now obtain the current-voltage characteristics of the cell by decomposing the integral in (6) to an electro-neutral and Debye-layer contributions,

$$\int_0^1 e \, dx = \int_0^1 \bar{e} \, d\bar{x} + \int_0^\infty E \, dX - \int_0^\infty \tilde{E} \, dX. \quad (54)$$

The outer voltage is calculated using (20),

$$\int_0^1 \bar{e} \, d\bar{x} = \ln \frac{1-j}{1+j}, \quad (55)$$

while the cathodic-layer voltage is calculated using (27),

$$\int_0^\infty E \, dX = -2 \ln \coth \{ (G/8)^{1/2} X_0 \}, \quad (56)$$

with a similar expression obtained for the anodic-layer voltage, wherein  $G$  and  $X_0$  are replaced by  $G + 4j$  and  $\tilde{X}_0$ . Using (37) together with (49)–(51) then furnishes the current–voltage relation

$$V = \ln j + 2 \ln \{g(j)\} - 2 \ln(1-j) - \ln p - 2 \ln \delta, \quad (57)$$

where the logarithmic term is contributed by cathodic-layer voltage. For  $j \ll 1$ , where  $g(j) \approx 2j$ , we obtain  $j \approx \delta^{2/3} e^{V/3} (p/4)^{1/3}$ , in accordance with [17].

The functional relation (57) implies that  $j$ , as a function of  $V$ , does not approach a limit as  $\delta \rightarrow 0$ . This explains the scatter of the distinct sets of data points in Fig. 1, corresponding to small but different  $\delta$  values. Note however that  $j$  becomes a function of  $V + 2 \ln \delta$  at that limit. In Fig. 3 we accordingly re-plot in the numerical data of Fig. 1 in the  $(V + 2 \ln \delta, j)$ -plane. The data clearly collapses on a single curve, which coincides with the approximate relation (57).

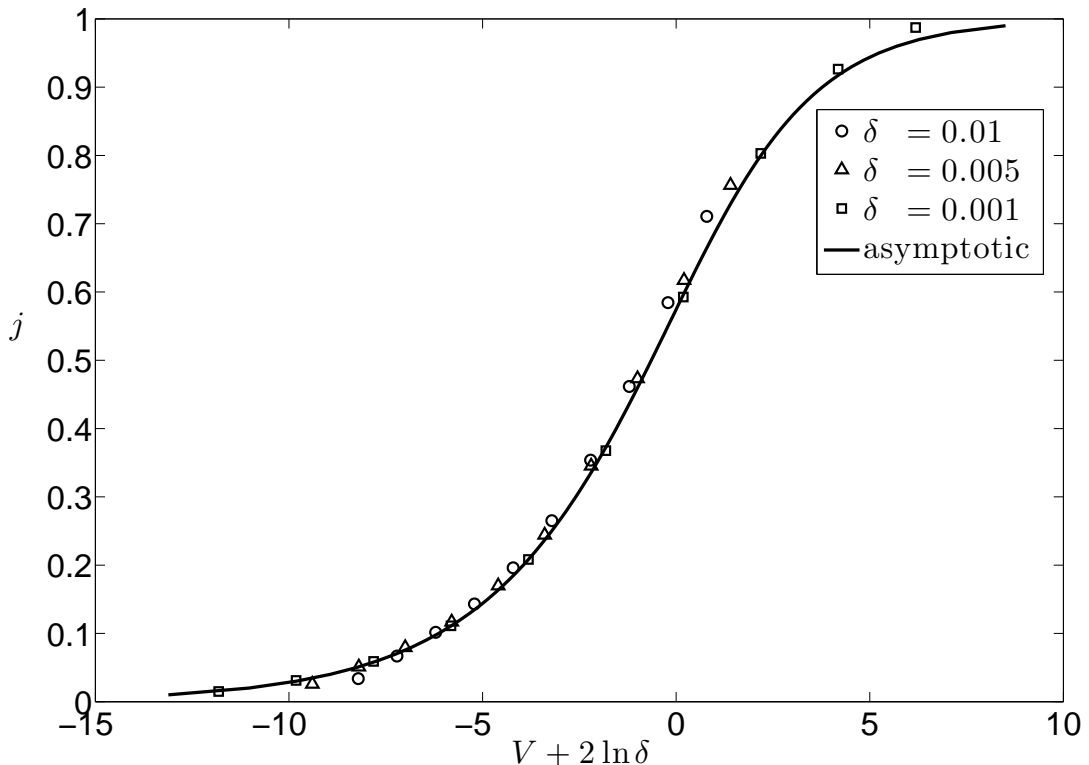


FIG. 3. Universal current–voltage characteristics. The data points of Fig. 1 are re-plotted on the  $(V + 2 \ln \delta, j)$ -plane. The solid line depicts the analytic approximation (57).

### B. Internal boundary layer

The logarithmically large voltage is associated with the anomalous structure of cathodic layer, wherein inert cationic concentration transforms from moderate  $O(1)$  values to large  $O(\delta^{-2})$  values near the cathode. The electric field undergoes a comparable transformation, from  $O(\delta^{-1})$  to  $O(\delta^{-2})$ . This transition reflects the emergence of an internal boundary layer, of width  $O(\delta^2)$ , within the  $O(\delta)$ -thick cathodic Debye layer. For  $x = O(\delta^2)$  we obtain the sublayer fields by expanding (27)–(30) for  $X = O(\delta)$ , in conjunction with (49)–(50). Defining the sublayer scaled coordinate [cf. (49)]

$$\xi = x/\delta^2 \quad (58)$$

we readily obtain the leading-order behavior

$$e = \delta^{-2}\mathcal{E}(\xi), \quad c_+ = \delta^{-2}\mathcal{C}_+, \quad c_- = \delta^2\mathcal{C}_-(\xi), \quad r = \mathcal{R}(\xi), \quad (59)$$

wherein

$$\mathcal{E} = -\frac{2}{\xi + \xi_0}, \quad \mathcal{C}_+ = \frac{4}{(\xi + \xi_0)^2}, \quad \mathcal{R} = p \frac{\xi_0^2}{(\xi + \xi_0)^2}, \quad (60)$$

and  $\mathcal{C}_- = (1 - j)^2 / \mathcal{C}_+$  [see (53)].

In Fig. 4 we present a comparison between the numerically calculated ionic concentrations and the above sublayer approximations for the same values of governing parameters as in Fig. 2. The logarithmic scale aids in focusing upon the near-cathode region and in capturing the disparate scales of the various concentrations.

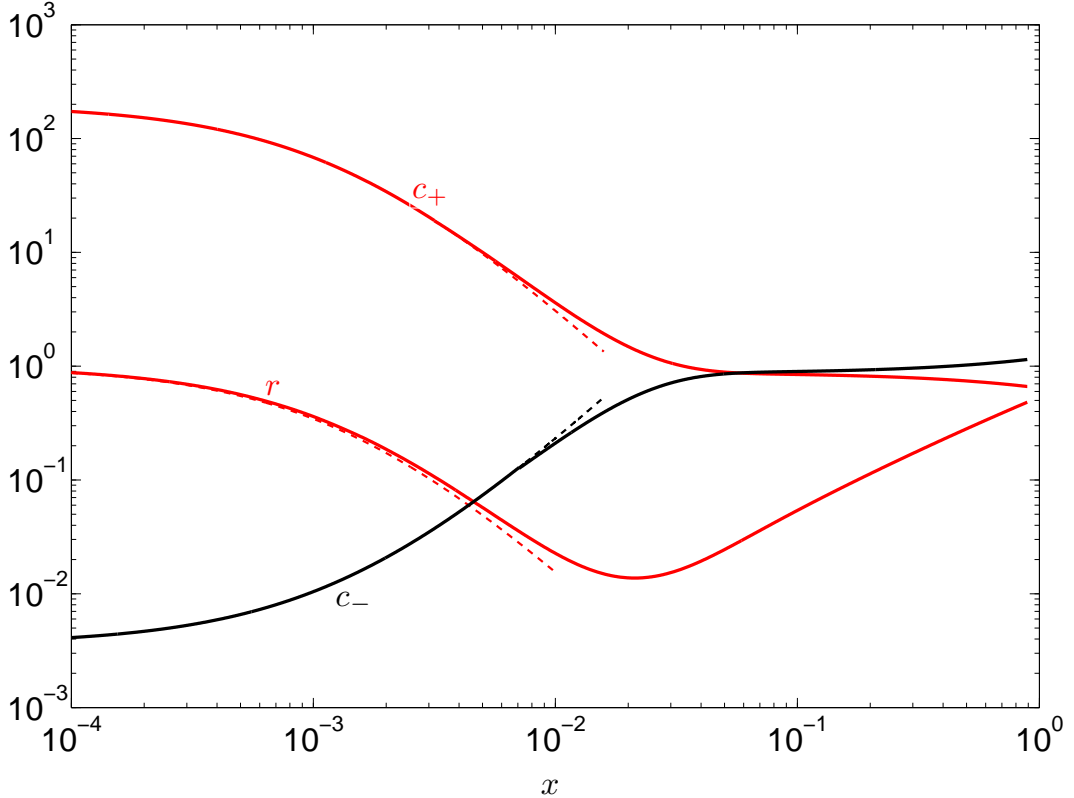


FIG. 4. Ionic concentrations in the cathodic Debye layer, obtained from numerical calculations (solid) and corresponding sub-layer approximations (dashed), obtained from (59). The governing parameters are the same as in Fig. 2 ( $\delta = 0.01$ ,  $p = 1$ ,  $V = 5$ ).

The  $O(\delta^{-2})$  field scaling near the cathode implies that the term  $-2\delta^2 e(x=0)$  in (16) transforms from  $O(\delta)$  to  $O(1)$ . Indeed, substitution of (25), (27) and (49) yields for it  $4/\xi_0$  at leading order. This initially appears to contradict (39). However, the integral term

appearing in (16),

$$-\delta^2 \int_0^1 e^2 dx,$$

originally estimated  $O(\delta)$  due to the two Debye-layer contributions, requires a renewed consideration as well. In view of its transformation, the cathodic Debye layer contribution now becomes, using (23), (25) and (27),

$$-\delta \int_0^\infty E^2 dX = 2^{3/2} G^{1/2} \delta \{1 - \coth(2^{-1/2} G^{1/2} X_0)\}.$$

Substitution of (49) yields at leading order  $-4/\xi_0$ . [The anodic Debye-layer contribution remains  $O(\delta)$ .] Thus, the  $O(1)$  contributions of the above two terms mutually cancel, reconfirming the validity of (39).

## VI. CONCLUDING REMARKS

In prevailing thin-Debye-layer analyses of ternary systems [15] the assumption of different initial amounts of inert ions leads to an asymptotic structure which resembles that of binary systems [11]. While that assumption may represent certain chemical reactions in ternary systems, it appears that the simplest and most natural case to study is that of identical amounts, corresponding to the presumed initial generation of inert ions by salt dissolution.

A naive attempt to analyze this problem using the familiar asymptotic expansions of binary systems [11] leads to the non-physical prediction of negative ionic concentrations. Moreover, concomitant numerical simulations indicate that the current–voltage curves corresponding to different Debye lengths do not approach a limit as that parameter vanishes. This behavior is in contrast with that appropriate for binary solutions [11].

Careful inspection of the numerical results indicates that the inert cations possess unusually large concentrations near the cathode, in contrast to the classical Debye-layer scaling. A revised asymptotic analysis using generalized asymptotic expansions uncovers a nonconventional structure, with asymptotic amplification of both electric field and inert cation concentration within the cathodic Debye layer. The generalized form of the cathodic boundary layer represents the emergence of an internal boundary sublayer.

The intensive electric field within the sublayer leads to a logarithmic scaling of the voltage with Debye width. This scaling is recast into a universal current–voltage relation. In the appropriate scaling, the numerically evaluated current–voltage curves collapse onto the

respective universal curve, which is in excellent agreement with the derived asymptotic approximation.

The present contribution addresses the asymptotic limit of thin double layers and moderate electric currents. Together with our previous paper [17], which has considered the complementary problem of moderate voltages and small currents, it provides a systematic analysis of ionic currents in supporting-electrolyte systems for identical number of inert ions. Both papers predict surprising behavior, unfamiliar from comparable investigations of binary system. While unconventional cathodic Debye-layer structure was already identified in the past for binary systems [20], it was in the context of currents exceeding the diffusion limit. The results of the present paper are all in the scope of under-limiting currents. The analysis of supporting-electrolyte systems at over-limiting currents, following [10, 20, 21], would constitute the natural next step for understanding these systems at the entire spectrum of applied voltages.

For convenience, we have performed our calculations using what may be the simplest description of ion exchange, assuming ideal ion-selective membranes. The description of more realistic systems requires appropriate modeling of cation exchange at the bounding surfaces. Typically, the generation and consumption of reactive ions is expressed through a redox expression, consisting of a forward deposition term (linear in the cationic concentration at the ion-exchange surface) and a backward dissolution term (independent of that concentration), biased by an exponential dependence upon the surface over-potential [1].

Another desired extension of the present analysis involves finite-size effects. When considering real systems, where the typical salt concentration is on the order of 0.1 to 1 moles per liter, the overcrowding of inert cations at the cathode becomes unphysical, with the  $O(\delta^2)$  thickness of the inner layer becoming sub-atomic. In principle, this would call for a more sophisticated continuum model which incorporates steric effects [22].

- 
- [1] J. S. Newman, *Electrochemical Systems* (Prentice-Hall, Englewood Cliffs, N. J., 1973).
  - [2] J. M. Tarascon and M. Armand, *Nature* **414**, 359 (2001).
  - [3] V. Barcion, D. P. Chen, and R. S. Eisenberg, *SIAM J. Appl. Math.* **52**, 1405 (1992), ISSN 0036-1399.

- [4] I. Rubinstein and B. Zaltzman, *Math. Models Methods Appl. Sci.* **11**, 263 (2001).
- [5] G. Yossifon, Y. C. Chang, and H.-C. Chang, *Phys. Rev. Lett.* **103**, 154502 (2009).
- [6] G. Yossifon, P. Mushenheim, Y. C. Chang, and H.-C. Chang, *Phys. Rev. E* **79**, 046305 (2009).
- [7] Y. Ben and H.-C. Chang, *J. Fluid Mech.* **461**, 229 (2002).
- [8] Y. Ben, E. A. Demekhin, and H.-C. Chang, *J. Colloid Interface Sci.* **276**, 483 (2004).
- [9] I. Rubinstein, B. Zaltzman, and I. Lerman, *Phys. Rev. E* **72**, 011505 (2005).
- [10] B. Zaltzman and I. Rubinstein, *J. Fluid Mech.* **579**, 173 (2007).
- [11] M. Z. Bazant, K. T. Chu, and B. J. Bayly, *SIAM J. Appl. Math.* **65**, 1463 (2005).
- [12] W. Nernst, *Z. Phys. Chem* **47**, 52 (1904).
- [13] M. Trau, D. A. Saville, and I. A. Aksay, *Langmuir* **13**, 6375 (1997).
- [14] A. V. Sokirko and F. H. Bark, *Electrochim. Acta* **40**, 1983 (1995).
- [15] M. van Soestbergen, *Electrochimica Acta* **55**, 1848 (2010).
- [16] V. G. Levich, *Physicochemical Hydrodynamics* (Prentice-Hall, Englewood Cliffs, N.J., 1962).
- [17] E. Yariv and Y. Almog, *Phys. Rev. Lett.* **105**, 176101 (2010).
- [18] We follow here the useful notation of Ref. [11].
- [19] D. C. Prieve, *Colloid Surface A* **250**, 67 (2004).
- [20] K. T. Chu and M. Z. Bazant, *SIAM J. Appl. Math.* **65**, 1485 (2005).
- [21] E. Yariv, *Phys. Rev. E* **80**, 051201 (2009).
- [22] I. Borukhov, D. Andelman, and H. Orland, *Phys. Rev. Lett.* **79**, 435 (1997).